Semiconductor/Polymer Nanocomposites of Acrylates and Nanocrystalline Silicon by Laser-Induced Thermal Polymerization

Frank Deubel, Marin Steenackers, José A. Garrido, Martin Stutzmann, Rainer Jordan*

In this work, a novel method for the preparation of polymer/semiconductor nanocomposites is presented. The nanocomposite is directly prepared from a suspension of nanocrystalline silicon (nc-Si) in bulk vinyl monomers (acrylates) and focused heating of the nc-Si by irradiation with a pulsed laser at 532 nm wavelength. The silicon nanocrystals are the inorganic component of the composite and simultaneously act as initiation points of the free radical polymerization forming the hybrid composite. By this method, patterned nanocomposite films with thicknesses up to ≈250 μm can be readily prepared. Furthermore, the polymerization kinetics were investigated for different reaction conditions such as irradiation time, laser intensity, nc-Si content, and addition of radical initiators.

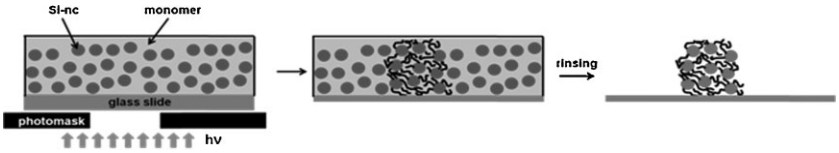

1. Introduction

Nanoparticle/polymer nanocomposites are an intriguing class of matter as they show unique electronic and optical properties because of the nanoscale particles in an organic matrix.[1] Especially the incorporation silicon nanocrystals as the inorganic component allows the preparation of high refractive index nanocomposites.[2] Different semiconductor nanoparticles, such as TiO_2, ZnO, and ZrO_2 have already been incorporated into bulk polymers to modulate the refractive index of the nanocomposites significantly.[3–6] The conventional approach for the synthesis of photocurable organic–inorganic nanocomposites involves a multifunctional monomer, a photoinitiator, the nanocrystals, and often an additional photosensitizer for UV–Vis curing.[6–10] Since the initiation of the polymerization occurs, not in direct proximity of the nanoparticles, but somewhere in the liquid phase, the change of the phase density results in a separation of the solid nanoparticles from the crosslinking polymer matrix.[11] This limits the amount of semiconductor nanocrystals that can be incorporated in the nanocomposite and hence the resulting refractive index differ within these areas. Thus, in other approaches the polymerization reaction is initiated directly at the nanoparticle surface using self-assembled monolayers to ensure a close incorporation of the particles to the polymer.[12–14]

Due to their high bulk refractive index, silicon nanocrystals are promising candidates for the design of high refractive index nanocomposites. Examples for the synthesis of nanocrystalline silicon (nc-Si) polymer

F. Deubel, M. Steenackers, Prof. R. Jordan
WACKER-Lehrstuhl für Makromolekulare Chemie, Department Chemie, Technische Universität München, Lichtenbergstr. 4, 85748 Garching, Germany
E-mail: rainer.jordan@tu-dresden.de
J. A. Garrido, M. Stutzmann
Walter Schottky Institut, Physik-Department, Technische Universität München, Am Coulombwall 3, 85748 Garching, Germany
Prof. R. Jordan
Professur für Makromolekulare Chemie, Department Chemie, Technische Universität Dresden, Zellescher Weg 19, 01069 Dresden, Germany

DOI: 10.1002/mame.201200392

nanocomposites are blending nc-Si into a gelatin matrix or UV-induced curing of a photopolymerizable system in the presence of H-terminated nc-Si.[15,16]

In our approach, nc-Si ($d = 20$ nm) is used, not only as the inorganic component, but acts simultaneously as the initiation site for the crosslinking polymerization. This is achieved by irradiation with green pulsed laser light ($\lambda = 532$ nm) at which the nc-Si become hot-spots in the bulk monomer medium. This route has two significant advantages over the conventional methods used so far: an improved absorption of nc-Si in the near IR and visible spectral range facilitates direct photopolymerization of the monomers without use of photoinitiators/photosensitizers. Moreover, enhanced patterning resolution and contrast can be achieved since the initiation of the polymerization occurs in direct vicinity of the nc-Si. In previous work it was shown that that films of spin-coated nc-Si can be annealed by laser-induced heating.[17] Heat dissipation is strongly limited in nc-Si because of steric constraints and nc-Si are eventually sintered and molten if heat is not readily dissipated. Dispersed nc-Si in a medium containing autopolymerizable monomers such as acrylates should act as confined local heating spots upon laser irradiation and should initiate a free radical polymerization by thermal autopolymerization and crosslinking.[18,19] Unlike surface-initiated polymerizations (SIPs)[20] involving surface-bond initiators or the self-initiated photografting and photopolymerization (SIPGP),[21] the polymerization should not result in direct grafting but thermal initiation of the autopolymerization in the bulk monomer phase. The formation of nc-Si/polymer nanocomposites was investigated including ex situ kinetic ^{1}H NMR measurements to determine the monomer conversion. Moreover, conditions for the creation of patterned nanocomposites were optimized and the effect of additional radical initiatiors [*N*,*N*-azobisisobutyronitril (AIBN)] investigated since patterning adds additional functionality to the materials.[22,23]

2. Experimental Section

All solvents were of analytical grade and obtained from Sigma–Aldrich (Steinheim, Germany). The monomers 2-hydroxyethyl acrylate (HEA) and ethylene glycol dimethacrylate (EGDMA) were from the same provider. Inhibitor was removed using basic alumina and the monomers were distilled and stored under dry nitrogen prior use. Microwave plasma-produced p-doped nc-Si particles (nc-Si, 1×10^{13} cm^{-3} boron) with an average diameter of 20 nm were obtained from Evonik.

Dispersions of nc-Si were prepared by 15 min ultrasonication of a desired amount of nc-Si in bulk monomer under dry nitrogen. The dispersions were additionally degassed via three freeze–pump–thaw cycles.

For photopatterning, the dispersions were put into a homemade irradiation chamber and irradiated through a photomask positioned over a thin glass slide that was cleaned from organic residues with a freshly prepared piranha solution (Caution!). Standard TEM grids were use as a photomask. Laser irradiation was performed with a pulsed (9 Hz) Nd:YAG laser at a wavelength of 532 nm. The size of the irradiated area was 5 mm × 5 mm.

After irradiation, the glass slide with the nanocomposite was immersed into fresh acetone and excessively rinsed with acetone and blow-dried with a jet of nitrogen.

Structure feature heights were determined by confocal microscopy on a Nanofocus μsurf confocal microscope and evaluated using μsurf software.

NMR spectroscopy was performed on a Bruker ARX 300 NMR spectrometer (300 MHz). The residual ^{1}H-signal of deuterated dimethyl sulfoxide (DMSO-d_6, $\delta = 2.50$ ppm) was used as an internal standard. 20 μL of a dispersion of nc-Si in HEA were filled into an NMR tube, sealed with a septum and degassed by three freeze–thaw cycles. The NMR tube was irradiated at a fixed laser intensity for different time periods. After irradiation, the partially polymerized dispersion was diluted with 600 μL DMSO-d_6. ^{1}H NMR spectra were recorded and the integrals under the vinyl protons of HEA were determined and normalized over the olefinic protons of an unreacted reference sample of the same batch. Conversion of the olefinic protons of the sample was calculated in %.

3. Results and Discussion

Figure 1a–c outlines the process of the initiator-free laser-induced polymerization of vinyl monomers. For a first proof of concept of this approach, nc-Si was dispersed in bulk EGDMA bearing two polymerizable groups, degassed and irradiated with pulsed laser light at through a photomask for 2 min ($f = 9$ Hz, $\lambda = 532$ nm, $I = 50$ mJ). After irradiation, the glass slide was removed from the reaction chamber and thoroughly cleaned with a good solvent for residual monomer or incompletely crosslinked poly(ethylene glycol dimethacrylate) (PEGDMA) fractions. As apparent from the optical (Figure 1d) and confocal (Figure 1e) microscope images, the crosslinking reaction is confined to the irradiated areas defined by the mask and the non-irradiated dispersion was selectively removed by the solvent, resulting in patterned nc-Si/PEGDMA nanocomposites.

Analog control experiments with nc-Si dispersed in pure ethanol as well as EGDMA monomer without dispersed nc-Si were performed. Both series of experiments did not result in any patterned material, indicating that neither dispersed nc-Si alone do not sinter into a closed film under these conditions nor the pure monomer could be polymerized and crosslinked by the laser irradiation. As nc-Si strongly adsorbs the laser light and is considerably heated,[17] it is most likely that the nc-Si dispersed in the monomer induce thermally induced autopolymerization[18,19] and crosslinking of the difunctional EGDMA directly resulting in a confined (patterned) nc-Si/PEGDMA nanocomposite. Crosslinking can be induced either by conventional methods such as the use of a difunctional

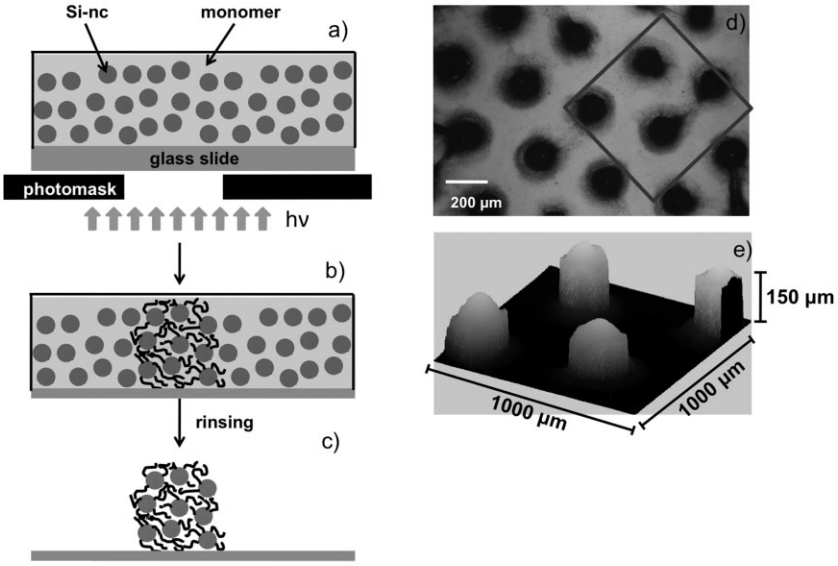

Figure 1. Schematic of the photolithography process (a–c) and resulting patterned nanocomposite films (d, e). (a) Irradiation of silicon nanocrystals dispersed in EGDMA with pulsed laser light at $\lambda = 532$ nm through a photomask results in the (b) confined formation of nanocomposites in a crosslinked polymer matrix. (c) Rinsing with a good solvent (acetone) gave patterned nanocomposite films. Optical (d) and confocal (e) microscope image of the patterned areas revealed well resolved patterns with a layer thickness of up to $h = 250$ µm.

acrylate monomer or by multiple covalent attachment of the polymer to the silicon nanocrystals. The stability of the incorporation of nc-Si within the polymer matrix was studied extensively. Neither intense sonication of the nanocomposite in good solvents nor long-term extraction (Soxhlet-extraction) resulted in measurable extractable amounts of components. We therefore assume a stable covalent bonding between the nc-Si particles and the polymer matrix. This was further corroborated by SEM studies that showed a good and homogeneous dispersion of the nc-Si particles in the composite (data not shown).

3.1. Patterned Nanocomposite Films

After proving the general feasibility of this technique, a first systematic study on the pattern quality was conducted to examine the pattern resolution, height, and stability of the structures as a function of the amount of dispersed nc-Si, irradiation time and intensity. Unless stated otherwise, an irradiation intensity of 50 mJ · cm^{-2} was used for all experiments. This value was found to be sufficient to generate stable and homogeneous polymer nanocomposites and patterning while avoiding unwanted thermal and/or photochemical decomposition.

The above-mentioned control experiments showed that the nc-Si particles play a crucial role for the crosslinking reaction. Variation of the amount of nc-Si in the dispersion revealed that a minimum of about 0.2–0.3 wt% nc-Si is needed to obtain morphologically stable nanocomposite patterns (Figure 2). From dispersions with nc-Si amounts, below this content some patterns could be observed by optical microscopy. However, with acetone, the patterns could be readily removed from the glass slides without noticeable remaining residues. With dispersions containing more than 0.6 wt% nc-Si, surface immobilized patterned nanocomposites were obtained but only of limited height of the individual structures (below 100 nm). This can be explained by the strong adsorption of the nc-Si particles limiting the penetration depth of the laser light into the dispersion. Optimal nc-Si contents between 0.3 and 0.5 wt% nc-Si in the bulk monomer could be identified that resulted in stable patterns immobilized on the glass slides.

Figure 3 shows a selection of confocal optical images of pattern nanocomposite films obtained for different irradiation times and particle concentrations. As judged from the pattern morphology and stability, we found optimal, or close to optimal conditions to be 0.45 wt% nc-Si for at least 45 s irradiation at $I = 50$ mJ · cm^{-2}. . However, to obtain thicker nanocomposite layers, considerably longer irradiation times of up to 6 min are realizable with nc-Si contents between 0.3 and 0.5 wt.-%. As shown in Figure 2, maximum nanocomposites layer thicknesses up to 250 µm can be realized in a reproducible fashion. Again higher nc-Si content and/or longer irradia-

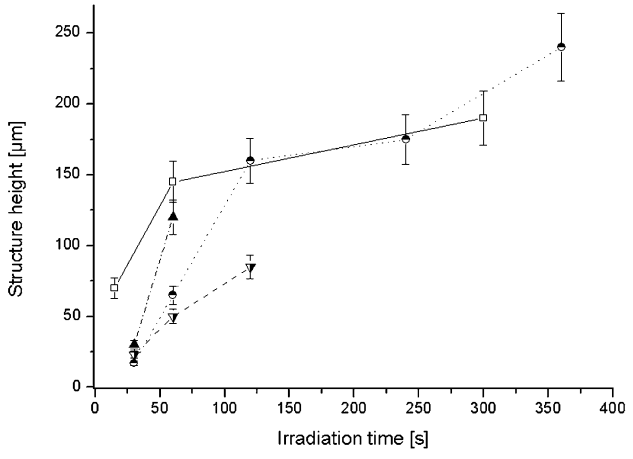

Figure 2. Obtained structure height as a function of irradiation time for particle concentrations of 0.3 wt% (black), 0.4 wt% (red), 0.5 wt% (green), and 0.6 wt% (blue).

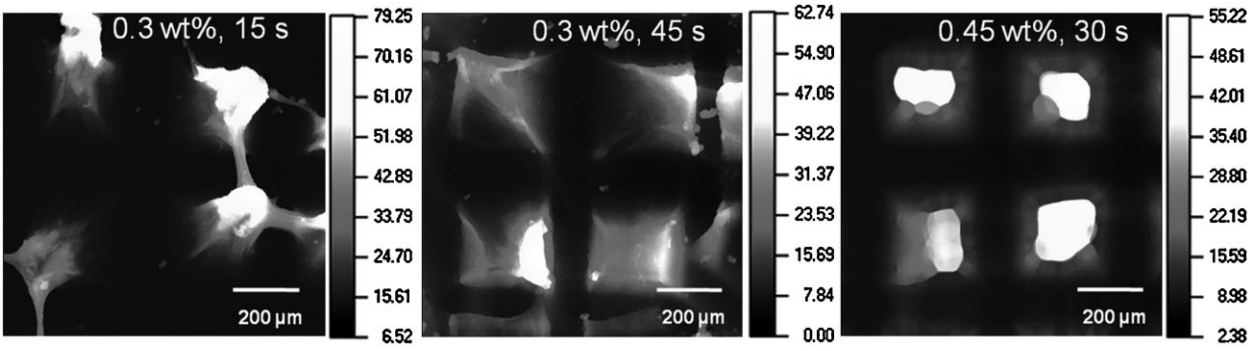

Figure 3. Confocal microscopy images of patterns obtained by irradiation of nc-Si dispersed in bulk EGDMA for different irradiation times ($I = 50\ mJ \cdot cm^{-2}$). The black/white coding represents the relative height in µm.

tion times with sufficient nanoparticle contents did not yield patterns of satisfying quality. Here, the formation of gas at the nc-Si/monomer interface was found to be a limiting factor. Thus, for the following experiments, dispersions of 0.3 wt% nanoparticles in bulk monomer, an irradiation period of 6 min at $I = 50\ mJ \cdot cm^{-2}$ was found to give stable and well-resolved patterns with feature heights over 200 µm height.

3.2. Ex Situ Kinetic Studies

In order to get a first insight of the monomer conversion of the polymerization the monofunctional analog to EGDMA, HEA was used as monomer to obtain mostly linear and soluble polymers and not a crosslinked matrix to enable a better analysis by means of ex situ NMR spectroscopy.[24] The HEA/nc-Si dispersions with 0.3 wt% particle content were degassed and irradiated directly in an NMR tube for different time periods from 0 to 15 min using a laser intensity of $50\ mJ \cdot cm^{-2}$. After irradiation, the dispersions were diluted with DMSO-d_6. Monomer conversion was calculated in % from the integral ratio of the vinyl protons to the respective PHEA polymer signals. The results are summarized in Figure 4a. Within 15 min, monomer conversion generally increases with increasing irradiation time. However, even after 15 min only 40% of the monomer was polymerized which is low compared to common photopolymerization methods using molecular photoinitiators. This might explain the above-described possibility of patterning of the nc-Si/monomer dispersions resulting in relatively well-resolved patterned nanocomposite films. Furthermore, the influence of the laser intensity was investigated with otherwise unchanged reaction conditions.

Figure 4b summarizes the development of the monomer conversion with the irradiation time from 0 to 12 min for two sets of experiments using 40 and $60\ mJ \cdot cm^{-2}$ laser intensity. Again, with increase of the irradiation time, increasing monomer conversions were found. Additionally, a higher laser intensity resulted in a slightly higher

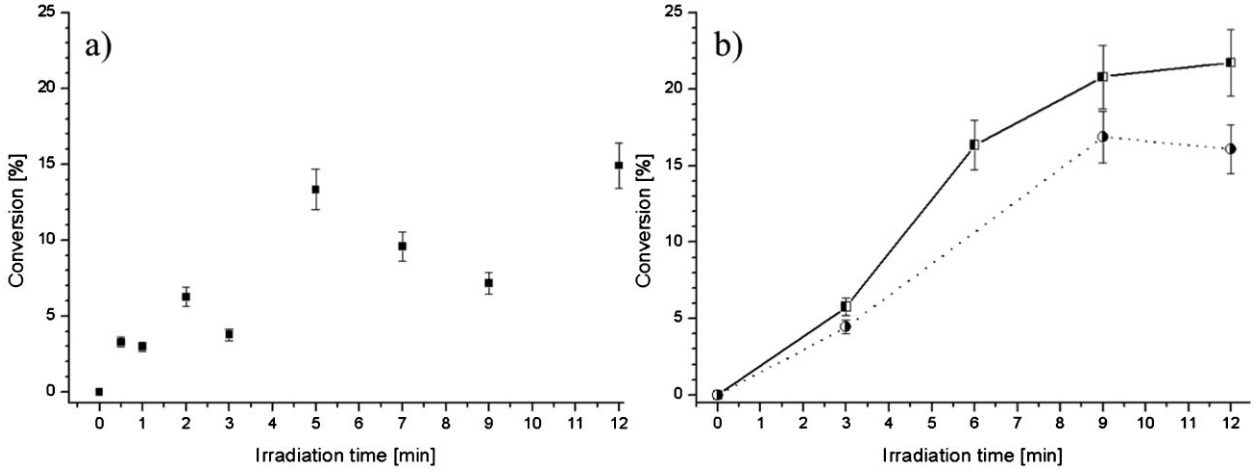

Figure 4. (a) Monomer conversion of a 0.3 wt% dispersion of nc-Si in bulk HEA as a function of the irradiation time ($I = 50\ mJ \cdot cm^{-2}$) and (b) monomer conversion in % of a 0.3 wt% dispersion of nc-Si in bulk HEA as a function of the irradiation time for $I = 40\ mJ \cdot cm^{-2}$ (dots) and $60\ mJ \cdot cm^{-2}$ (squares).

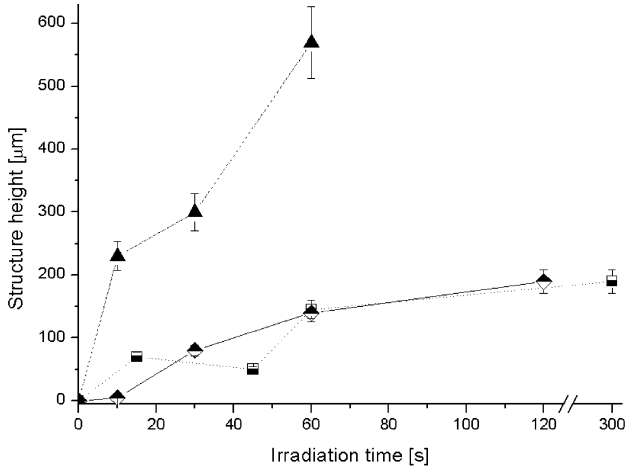

Figure 5. Nanocomposite layer thickness as a function of the irradiation time for dispersions of 0.3 wt% Si-nc in bulk EGDMA containing no (squares), 0.71 wt% (diamonds) and 1.3 wt% AIBN (triangles).

monomer conversion. However, an increase of the laser intensity close or above 100 $mJ \cdot cm^{-2}$ (data not shown) resulted in no significant improvement of the monomer conversion but in significant decomposition of the organic components along with nanocomposite formation.

3.3. Addition of Initiator

Although the polymer matrix formation is well confined to the irradiated areas, the relatively low monomer conversion as determined by NMR spectroscopy with the monofunctional acrylate system calls for optimization. Addition of a common radical initiator that composes thermally should improve the radical polymerization reaction and formation of a crosslinked matrix around the nc-Si. Thus, AIBN was added to the dispersions containing 0.3 wt% of nc-Si particles in EGDMA monomer. The amount of AIBN in these dispersions were 0.71 and 1.43 wt%. For both cases stable and well resolved pattern nanocomposite films could be obtained, analog to experiments without AIBN. Hence, the addition of temperature labile radical initiator did not impair the patterning process at the investigated initiator concentrations. In Figure 5, the influence of the addition of AIBN upon the resulting nc-Si/PEGDMA nanocomposite film morphology is summarized. For dispersions containing 0.71 wt% AIBN, the laser irradiation through a photomask at $I = 50\ mJ \cdot cm^{-2}$ for up to 5 min yielded pattern with almost identical film thicknesses as compared to dispersions without AIBN. However, with 1.43 wt% AIBN added significant higher layer thicknesses up to 600 µm within only 2 min could be obtained.

Moreover, already by visual inspection the pattern quality appeared noticeably improved. This could be confirmed by optical microscopy as shown in Figure 6. While low AIBN concentrations reproduced the photomask as irregular patterned nanocomposite films, a higher AIBN content dramatically improved the pattern appearance and morphology as well as the layer thickness. Importantly, the photocrosslinking of the EGDMA was still confined to the irradiated areas and no continuous film formation was observed.

4. Conclusion

A direct approach for the preparation of hybrid organic–inorganic nanocomposites from a suspension of silicon nanocrystals (nc-Si) in bulk monomer to a crosslinked polymer matrix with homogeneously distributed silicon nanoparticles is presented. The function of the nc-Si is twofold: on one hand it is the inorganic component of the composite, on the other hand it converts the energy input in the form of laser irradiation into thermal energy that triggers the polymerization of acrylic monomer to form the crosslinked organic matrix. It can be assumed that the crosslinking is initiated in close vicinity of the nc-Si hot-spots. Irradiation of dispersions through photomask result in patterned nanocomposite film formation as the

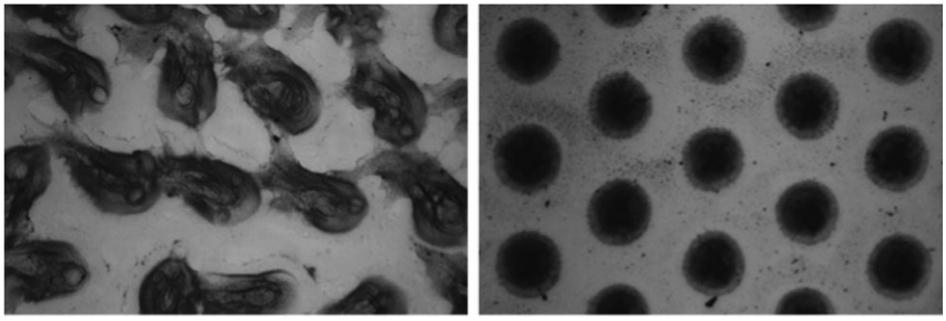

Figure 6. Optical microscopy images of patterned nanocomposite films prepared from dispersions without (left) and with (right) 1.43 wt% AIBN, irradiated at $I = 50\ mJ \cdot cm^{-2}$ for 30 s.

polymerization is locally confined. Layer thicknesses of up to 250 μm and well-resolved patterns were readily obtained. Reaction conditions could be optimized by the nc-Si content of the monomer-nanoparticle dispersion. The relatively slow polymerization reaction kinetics could be compensated by the addition of AIBN as a classical thermal initiator. This also significantly improved the pattern morphology as well as the realizable nanocomposite film thickness to around 600 μm.

The laser-induced thermal polymerization technique is a straightforward and easy-to-use method for the preparation of a broad range of novel materials in the area of, e.g., high refractive index nanocomposites or coatings containing silicon nanoparticles.

Acknowledgements: This work was financially supported by the WACKER Chemie AG through Ph.D. and postdoctoral scholarships of the WACKER-Institute of Silicon Chemistry at the Technische Universität München for F.D. and M.S. R.J. further acknowledges support by the excellence-cluster "Center for Advancing Electronics Dresden" (cfAED) at the Technische Universität Dresden.

Received: October 24, 2012; Revised: November 23, 2012; Published online: January 21, 2013; DOI: 10.1002/mame.201200392

Keywords: nanocomposites; nanoparticles; patterning; photopolymerization; silicon nanocrystals

[1] P. M. Ajayan, L. S. Schadler, P. V. Braun, *Nanocomposite Science and Technology*, Wiley-VCH, Weinheim **2003**.
[2] C. L. Lu, B. Yang, *J. Mater. Chem.* **2009**, *19*, 2884.
[3] C. C. Chang, W. C. Chen, *J. Polym. Sci., Part A: Polym. Chem.* **2001**, *39*, 3419.
[4] E. Reck, S. Seymour, *Macromol. Symp.* **2002**, *187*, 707.
[5] US 6656990 (2003) invs.: P. J. Shustack, Z. K. Wang.
[6] N. Suzuki, Y. Tomita, *Opt. Express* **2006**, *14*, 12712.
[7] C. Lü, Z. Cui, Y. Wang, Z. Li, C. Guan, B. Yang, J. Shen, *J. Mater. Chem.* **2003**, *13*, 2189.
[8] S. Zhou, L. Wu, *Macromol. Chem. Phys.* **2008**, *209*, 1170.
[9] S. Scholz, S. Kaskel, *J. Colloid Interface Sci.* **2008**, *323*, 84.
[10] Y. Zhao, F. Wang, Q. Fu, W. Shi, *Prog. Polym. Sci.* **2007**, *48*, 2853.
[11] F. del Monte, O. Martínez, J. A. Rodrigo, M. L. Calvo, P. Cheben, *Adv. Mater.* **2006**, *18*, 2014.
[12] R. Jordan, N. West, A. Ulman, Y. M. Chou, O. Nuyken, *Macromolecules* **2001**, *34*, 1606.
[13] Q. Zhou, S. Wang, X. Fan, R. Advincula, J. Mays, *Langmuir* **2002**, *18*, 3324.
[14] S. Nuss, H. Bottcher, H. Wurm, M. L. Hallensleben, *Angew. Chem., Int. Ed.* **2001**, *40*, 4016.
[15] F. Papadimitrakopoulos, P. Wisniecki, D. E. Bhagwagar, *Chem. Mater.* **1997**, *9*, 2928.
[16] R. Souane, J. Lalevee, X. Allonas, J. P. Fouassier, *Macromol. Mater. Eng.* **2010**, *295*, 351.
[17] R. Lechner, A. R. Stegner, R. N. Pereira, R. Dietmüller, M. S. Brandt, A. Ebbers, M. Trocha, H. Wiggers, M. Stutzmann, *J. Appl. Phys.* **2008**, *104*, 053701.
[18] P. J. Flory, *J. Am. Chem. Soc.* **1937**, *59*, 241.
[19] H. J. L. Bressers, J. G. Kloosterboer, *Polym. Bull.* **1980**, *2*, 201.
[20] T. Chen, I. Amin, R. Jordan, *Chem. Soc. Rev.* **2012**, *41*, 3280.
[21] M. Steenackers, A. Küller, S. Stoycheva, M. Grunze, R. Jordan, *Langmuir* **2009**, *25*, 2225.
[22] Y. Y. Li, S. Kollengode, M. J. Sailor, *Adv. Mater.* **2005**, *17*, 1249.
[23] M. J. Ventura, M. Gu, *Adv. Mater.* **2008**, *20*, 1329.
[24] J. G. Kloosterboer, *Adv. Polym. Sci.* **1988**, *84*, 1.